Visible light responsive titania photocatalysts codoped by nitrogen and metal (Fe, Ni, Ag, or Pt) for remediation of aqueous pollutants

Hongqi Sun*, Guanliang Zhou, Shizhen Liu, Ha Ming Ang, Moses O Tadé, Shaobin Wang*

Department of Chemical Engineering and CRC for Contamination Assessment and Remediation of the Environment (CRC-CARE), Curtin University, GPO Box U1987, Perth, WA 6845, Australia

*Corresponding Author. Tel: +61 8 92663776, Fax: +61 8 92662681
E-mail address: shaobin.wang@curtin.edu.au (S. Wang); h.sun@curtin.edu.au (H. Sun)

ABSTRACT

Various cation and nitrogen doped and codoped TiO_2 photocatalysts, such as N-TiO_2, Pt-TiO_2, N-Fe-TiO_2, N-Ni-TiO_2, N-Ag-TiO_2 and N-Pt-TiO_2, were prepared by an acid-catalysed sol-gel process. The photocatalysts were characterised by X-ray diffraction (XRD), nitrogen adsorption-desorption isotherms, UV-visible diffuse reflectance absorption spectroscopy (UV-vis DRS), and X-ray photoelectron spectroscopy (XPS). The activities of the photocatalysts were evaluated in photodegradation of phenol solutions under simulated sunlight irradiations. A negative effect of some transition metals (iron and nickel) on photocatalysis was observed on N-metal codoped TiO_2, while enhancements in photocatalysis from noble metals (silver and platinum) were obtained. N-Pt codoped TiO_2 showed a higher activity under UV-vis irradiations than Degussa P25, with an enhancement of 5.9 times higher. The synergistic effect of N-Pt-codoping was ascribed to the multivalent states of platinum. In addition, photocatalytic activity of N-, Pt-doped and N-Pt-codoped materials were further investigated under visible light irradiations with $\lambda > 430$ nm and $\lambda > 490$ nm. This study therefore demonstrated a promising strategy for design of highly efficient photocatalysts for remediation of aqueous pollutants.

Keywords: Photocatalysis**;** TiO_2; Codoping; **V**isible light; Nitrogen; Transition metal; Noble metal; Phenol

1. Introduction

Semiconductor based photocatalysis has been recently manipulated in the visible light region since the remarkable success of modified titanium dioxide. Recently, Dionysiou et al. [1] presented a comprehensive review on the structure, properties and electronic structures of TiO_2 photocatalyst. The developments in the approaches for improving the visible light response of TiO_2 by non metal and/or metal doping, dye sensitizing and semiconductor coupling were discussed. Drogui et al. [2] summarized the recent development in environmental applications of TiO_2, with an emphasis on water and wastewater treatment by visible light photocatalysis. The mechanism of visible light photocatalysis for wastewater treatment, such as phenol photodegradation, was also discussed by identification of the intermediates and formation of hydroxyl radicals [3].

Among a variety of modifications, non-metal doping, i.e. nitrogen doping has demonstrated to be able to simultaneously increase the photocatalytic activities of TiO_2 under both ultraviolet (UV) and visible light irradiations [4, 5]. Owing to such a merit, along with its long-term stability and high efficiency, nitrogen doping was believed to be superior to transition metal doping in previous studies [6, 7]. However, the ongoing topics of nitrogen doping were still driven by the debates and controversies [8], leading to dramatically increasing investigations on the synthesis, characterisation, mechanism and photocatalytic performance. In general, synthesis of nitrogen doped TiO_2 (N-TiO_2) can be realised by two approaches, e.g. gas phase annealing and wet-chemical route. In gas phase synthesis, sputtering TiO_2 in N_2 (40%)/Ar and thermally treating TiO_2 in NH_3 (67%)/Ar were investigated by Asahi et al. [5]. Many other investigations, such as oxidative treatment [9, 10], microwave plasma-torch using gas-phase $TiCl_4$ [11], and chemical vapour deposition (CVD) [12], were also reported. On the other hand, wet-chemical methods have been proven as an effective strategy for synthesis of nitrogen doped TiO_2 as well. Hydrolysis with ammonia [13] or hydrazine hydrate [14-16], sol-gel process [17], hydrothermal method [18], and solvothermal route [19] have been employed to synthesise N-TiO_2. In the above methods, various preparation parameters, such as Ti precursor, nitrogen precursor, gas composition, applied current, solvent, reaction temperature/time, calcination temperature/time, and

post-treatment, were usually considered to affect structure and performance of the catalysts. The physicochemical properties of the resulting photocatalysts then vary from lab to lab, possibly leading to the wide controversies in the reason for visible response mechanism. The core in the debates has been the identification of effective dopants [20, 21], namely the chemical nature of the doped nitrogen contributing to the visible light response. Asahi et al. [5] reported that the substitutional doping of N would mix O *2p* state with N *p* states, leading to the band gap narrowing. But the molecularly existing dopants, such as NO and N_2, only provide the bonding states below the O *2p* valence bands and antibonding states deep in the band, thus would be unlikely effective for photocatalysis. The binding energy of substitutional N is generally located at ca. 397 eV from N-Ti-N. Later several investigations reported inconsistent findings to Asahi's theory [5, 22-27]. No substitutional N was observed, but a N binding energy at ca. 400 eV appeared. Oxygen-deficient structure [24], NH_x species [23], N-Ti-O linkage [26], and NO_x [14-16, 22, 25, 27] have been proposed to be the origins of visible light photocatalysis from N-TiO_2. By a combined experimental and theoretical approach, Livraghi et al. [20] proposed that N-TiO_2 contained single-atom nitrogen impurities, which formed either diamagnetic (N_b^-) or paramagnetic ($N_b^\bullet$) bulk centres, and that those N_b centres were responsible for visible light absorption. Mitoraj et al. [21] suggested that neither nitridic nor NO_x species nor defect states were responsible for visible light photocatalysis, but higher melamine condensation products acting as visible light sensitisers.

The authors previously reported that codoping is a promising strategy for the improved visible light photocatalytic activity [28]. Apart from the interests in the nature of doping, investigators also conducted metal or non-metal codoping with nitrogen for improved photocatalytic activity. Investigations on N-F [29], N-S [30, 31], N-C [32], and N-Br [33] codoping have been reported. However, codoping at two anionic sites might induce significant crystal distortion and charge unbalance, resulting in a high rate of carriers' recombination. Therefore, codoping by nitrogen and a metal ion would be a better choice. Zhang et al. [34] reported that nitrogen and nickel codoping would give rise to a synergistic effect which would improve the visible light photocatalytic activity. Parida and Naik [35] showed that the synergistic effect of iron and nitrogen greatly enhanced the photocatalytic activity for degradation of phenol under solar light. Yin et al. [36] proved that either platinum

or iron could improve the activity of N-TiO_2. Morikawa et al.[37] studied the photocatalytic oxidation of gaseous formic acid, acetic acid, acetaldehyde and toluene on several N-TiO_2 loaded with Fe, Cu or Pt catalysts, which were prepared by annealing TiO_2 in NH_3 followed by impregnation. Sreethawong et al. [38] reported the preparation of Pt/N-doped TiO_2 by three steps, including (i) preparation of TiO_2, (ii) nitrogen doping by calcination with urea, and (iii) Pt loading by the incipient wetness impregnation. Solymosi et al. [39] reported synthesis of noble metals, such as Pt, Pd, Ir, Rh, and Ru onto N-TiO_2 by impregnation, and found that deposition of Pt would significantly increase the activity in photocatalytic decomposition of methanol. Wu et al. [40] suggested silver as a good option for codoping TiO_2 with nitrogen. We recently reported N/Pt-TiO_2 showed much better activity in indoor air purification [41]. Various gaseous VOCs were decomposed in a batch reactor and toluene was degraded in a continuous phase under room lighting over the Pt/N-TiO_2 photocatalyst.

In general, the preparation method and the activity evaluation varied at each protocol, therefore a comprehensive investigation keeping identical conditions would be in demand. In this paper, we present three systematic studies, (a) Effect of metal ions (Fe, Ni, Ag and Pt) on the physicochemical properties of nitrogen doped TiO_2, (b) Effect of doping level of platinum (0, 0.5, and 1.0 at.%) on the physicochemical properties of nitrogen doped TiO_2, and (c) Effect of light sources (UV-visible, visible light > 430 nm and > 490 nm) on the photodegradation efficiency of organic pollutants. The mechanisms for the increased visible light absorption and photocatalytic activity were investigated.

2. Experimental

2.1. Preparation of codoped TiO_2 photocatalysts

An acid-catalysed sol-gel method was applied to synthesise various nitrogen-metal (Ni, Fe, Ag or Pt) codoped TiO_2 photocatalysts. A typical procedure of the synthesis was as follows. 100 mL of ethanol, 20 mL of acetic acid and 20 mL of titanium (IV) isopropoxide (TTIP, Aldrich, 97%) were mixed to produce *solution A*. 1 L of deionised water, 1 mL of HNO_3 (69.5%), a certain amount of metal precursors (iron (III) nitrate (98%), nickel (II) nitrate hexahydrate (98.5%), silver nitrate (99.0), or hexachloroplatinic acid (99.9%) from

Sigma-Aldrich, 15.547 g of urea (Ajax Finechem, 99%) and 20 mL of acetic acid were mixed as *solution B*. In an ice bath, *solution A* was added dropwise into *solution B* to carry out a controlled hydrolysis, and then aged for 48 h. The overall molar ratio of reagents for Ti precursor: metal precursor (Pt, Ag, Fe, or Ni): urea: acetic acid: nitric acid: ethanol in the mixed solution was 1: 0.01: 4.00: 10.64: 0.24: 26.12. After evaporation at 80 ^{o}C, the dried gels were annealed in air at 400 ^{o}C for 4 h unless specifically stated. Then a nitrogen and metal codoped TiO_2 photocatalyst was obtained. The prepared samples were labeled as N-M (*x*)-codoped TiO_2, where N was nitrogen (level as measurement), M was Pt, Ag, Fe or Ni, and *x* was the doping level of metal ions. Pure, nitrogen doped TiO_2, and Degussa P25 (TiO_2, 75% anatase and 25% rutile, 20 nm, and S_{BET} = 50 m^2/g) were used as reference samples for comparisons.

2.2. Characterisation of the photocatalysts

The crystalline structure of samples was analysed by powder X-ray diffraction (XRD) using a Bruker D8-Advance X-Ray diffractometer with Cu Kα radiation (λ = 1.5418 Å). UV-visible diffuse reflectance spectra (UV-vis DRS) of samples were recorded on a JASCO V-670 spectrophotometer with an Ø 60 mm integrating sphere, and $BaSO_4$ as a reference material. The Brunauer-Emmett-Teller (BET) surface area and pore size distribution were evaluated by nitrogen sorption at -196 ^{o}C using a Quantachrome Autosorb AS-1. Chemical compositions of the samples were analysed by X-ray photoelectron spectroscopy (XPS) using Thermo Escalab 250 with a monochromatic Al Kα X-ray source. All binding energies were calibrated by the C 1*s* peak at 284.6 eV.

2.3. Photocatalytic decomposition of pollutants

The aqueous oxidation of phenol was carried out in a 1-L of Pyrex double-jacket reactor. A water bath connected to a pump was used to maintain the reaction temperature at 30 ± 0.5 ^{o}C, and a magnetic stirrer was used to ensure the catalyst dispersed uniformly in reaction solutions. The irradiations were supplied by a MSR 575/2 metal halide lamp (575 W, Philips). Various cut-off filters were used to obtain the desired irradiations. At each set time interval, 1 mL solution was withdrawn by a syringe and filtered by a 0.25 μm Millipore film into a

HPLC (high performance liquid chromatography) vial for analysis. The concentration of phenol was analysed on a 380-LC HPLC (Varian, USA) with a UV detector set at $\lambda = 270$ nm. A C–18 column was used to separate the organics while the mobile phase of 30% CH_3CN and 70% water was flowing through the column at a flowrate of 1.5 mL/min.

3. Results and discussion

3.1. Crystal structure

Fig. 1 shows XRD patterns of pure and modified TiO_2 photocatalysts. It was found that all samples were of anatase phase, owing to the identical calcination of 400 ^oC for 4 h. Compared to highly crystalline anatase TiO_2, (103) and (112) crystal faces did not grow very well, which commonly occurred in the TiO_2 annealed below 500 ^oC. Fig. 1(A) shows that the intensities of (103) face of undoped, N-doped and N-Fe codoped TiO_2 were slightly higher than N-Ni-, Ni-Ag- and N-Pt-codoped TiO_2. Nonetheless, no obvious brookite phase (ca. 30 ^{o} of 2θ) was observed on all samples. Fig. 1(B) displays XRD patterns of Pt doped and N-Pt codoped TiO_2 at different levels of N. It was seen that Pt metallic phase was observed in Pt-doped sample at doping level of 1.0 at.%, while absence of metallic Pt in N-Pt codoped samples occurred. Such an observation might indicate that the codoping of N would retain Pt at ionic states.

The crystallite size and lattice parameters were calculated based on XRD profiles using the Scherrer formula and powder indexing, respectively [28], and the results are given in Table 1. The crystallite sizes of the catalyst samples were in a narrow region of 4.8 to 6.9 nm, mainly due to the acid-catalysed sol-gel process. Compared to 6.4 nm of undoped TiO_2, N-doping would increase the crystallite size of TiO_2. The incorporation of other metal ions would prohibit the crystalline growth, leading to a smaller size. Meanwhile, N-Pt codoped TiO_2 either at 0.5 at.% or 1.0 at.% Pt level had a smaller crystallite particle size than other samples. For the lattice parameters, *a* (or *b*) axis of all samples remained unchanged compared to undoped TiO_2. N-TiO_2 had a less *c* axis than undoped TiO_2 due to the smaller radius of N than O [28]. The substitution of Ti (IV) by other metal ions with smaller radii, along with a smaller crystallite size, led to the decreases in *c* axis [42]. Ni and Fe, which have slightly

smaller radii than Ti^{4+}, presented similar distortion, indicating the same level of substitutional doping. The ion radius of silver is too large to be doped, thus no significant change in codoping with nitrogen was observed. The distortion of N-Pt (1.0 at.%) was the largest among the samples, indicating an effective substitutional doping of Pt^{4+}. It is noteworthy that the element loading level was not the same as substitutionally doping level, and this point will be discussed in the following XPS analysis.

[Insert Fig. 1]

[Insert Table 1]

3.2. Textural structure

Fig.2 (A) presents N_2 adsorption-desorption isotherms of pure, N-doped, and N-Pt-codoped TiO_2 photocatalysts. The BET surface areas were found to be 46.6, 78.5 and 94.5 m^2/g, for pure, N-doped, and N-Pt-codoped TiO_2, respectively. It was reported that both N and Pt doping could increase the specific surface area of TiO_2 compared to bare sample [43, 44]. The highest BET surface area of N-Pt-codoped TiO_2 might be due to the the presence of urea, which leads to controlled nucleation and growth of nanocrystallites and also formation of mesoporous structure, and the platinum species on the surface which prevents aggregation. The pore volumes were 0.072, 0.224, and 0.084 cm^3/g, for pure, N-doped, and N-Pt-codoped TiO_2, respectively. Referring to the IUPAC classification, the adsorption isotherms of the samples were type IV and had a hysteresis loop of type H2. A hysteresis loop at p/p_o between 0.4 and 0.8 was observed in pure TiO_2, indicating the presence of a mesoporous structure. Since no templates were used, such a structure was possibly due to the organic Ti precursor and the acid-catalysed sol-gel process. The hysteresis loops of N- and N-Pt-TiO_2 were broadened at p/p_o between 0.3 and 0.9, owing to the broader pore size distribution of the doped samples. N-doped TiO_2 had some larger pores. The results suggested that both N doping and codoping of Pt would affect the porous structures of TiO_2 photocatalysts.

[Insert Fig. 2]

Fig. 2 (B) shows the pore size distributions of pure and modified TiO_2. Pure TiO_2 showed a

narrow pore size distribution centred at 4.3 nm, and up to 10 nm. N-TiO_2 had the largest pore volume, and its pore size distribution moved to a larger size of 7.8 nm, with a broad peak up to 40 nm. It was interesting to see that the N-Pt-TiO_2 had the smallest pores centred at 3.0 nm, but the size distribution was broader than pure TiO_2, up to 20 nm. The results clearly showed that either N or Pt would significantly influence the pore size and pore size distribution.

3.3. Optical properties and band gap energy

The absorption thresholds and band gap energies of pure and modified TiO_2 were evaluated by UV-vis DRS. Fig. 3 (A) shows the optical properties of various photocatalysts. Pure TiO_2 showed an absorption threshold at 406 nm, which was longer than the well-known anatase of 387 nm, due to the lower crystalline degree at calcination of 400 ^oC and carbon pollution from organic Ti precursor. N-doping only slightly extended the absorption threshold to 410 nm, but it produced a very strong absorption in visible light region up to 550 nm. Such an observation was well consistent with previous studies [14-16], because the doped N was not at substitutional sites, but on the surface. The incorporation of additional metal would significantly broaden the absorption edges of N-TiO_2. Moreover, the absorbance in visible light region was also improved by the codoping, except for N-Ag-TiO_2. Among these samples, N-Pt-TiO_2 had the longest absorption edge and the highest absorbance in visible light region. The strongest absorbance of Pt-TiO_2 in visible light region suggested that the extended absorption is mostly attributed to platinum modification. Previous studies have also proven that the visible light absorption of TiO_2 or N-TiO_2 could be significantly improved by metallic particles, oxides and salts of platinum [45, 46].

[Insert Fig. 3]

The band gap energies of the materials could be estimated using the following equation [47].

$$(\alpha h\nu)^n = B(h\nu - \mathrm{Eg}) \quad (1)$$

Where $h\nu$ is the photon energy, α is the absorption coefficient which can be obtained from the scattering and reflectance spectra according to the Kubelka-Munk theory, B is a constant relevant to the material and n is the value that depends on the nature of transition: 2 for a

direct allowed transition, 3/2 for direct forbidden transition, and 1/2 for indirect allowed transition. The $(\alpha h\nu)^n$ (n = 1/2) versus $h\nu$ extrapolated to α = 0 represents the absorption band gap energy. Fig. 3 (B) shows the band gap energies of the various TiO_2 photocatalysts. The pure TiO_2 had a band gap energy of 3.05 eV and N-TiO_2 showed a slight red-shift, giving a band gap of 3.02 eV. Pt-TiO_2 has a very low band gap energy of 2.57 eV. In terms of nitrogen and metal codoping, the band gap energies were 2.88, 2.68, 2.98, and 2.58 eV for N-Fe, N-Ni, N-Ag and N-Pt codoped TiO_2, respectively. It was found that Fe, Ni and Pt were able to further decrease the band gap of N-TiO_2. On the other hand, silver was not effective for narrowing the band gap, possibly due to the large radius of Ag^+, as shown in Table 1. Similar observations were also reported by Shang et al. [40], whose results demonstrated a slight improvement of visible light absorption from Ag to N-TiO_2, but no band gap narrowing.

3.4. XPS studies

Fig. 4 (A) shows XPS N1*s* spectra of pure, N-doped, and N-Pt-codoped TiO_2 photocatalysts. No obvious signal at 396 eV was observed, indicating no substitutional N doping was produced [5]. In N-doped and codoped samples, fitted peaks centred at 399.7 eV were observed. The position was well consistent with our previous studies [14-16, 41], indicating the presence of N-containing species, such as NO, NO_2, NO^{2-}, and NO_2^{2-}, etc. This type of N doping was typically seen in the samples from wet-chemical synthesis [22, 25, 27]. The N doping level in N-TiO_2 was detected to be 0.21 at.%, whereas 0.75 at.% for N-Pt-codoped TiO_2. It indicated that codoping with Pt would increase N doping level. Higashimoto et al. [48] reported that the ratios of N/Ti on N-TiO_2 and $PtCl_x$/N-TiO_2 were roughly estimated to be 0.34 and 0.29 at.%, respectively. But in their study, nitrogen doping was completed before adsorption of Pt salt, and there was no calcination afterward. Our study is the first observation in increased N doping level by Pt, possibly due to the interaction between the precursors in solution and calcination for maintaining charge balance [49].

[Insert Fig. 4]

Fig. 4(B) shows XPS Ti 2*p* spectra. It was found that Ti $2p_{3/2}$ of N-TiO_2 showed a red-shift of 0.42 eV to lower energy when compared to pure TiO_2. The shift to lower binding energy

generally implies a higher electron density. In modified TiO_2, higher energy density of Ti might be attributed to the presence of Ti^{3+} centre in N-TiO_2 [14]. Contrast to N-TiO_2, peak of Ti $2p_{3/2}$ in N-Pt-TiO_2 remained unchanged, owing to the charge balance from anion-cation codoping.

Fig. 4 (C) displays Pt 4*f* XPS spectra of N-Pt-TiO_2. Four peaks of Pt $4f_{7/2}$ were identified by curve devolution, implying that multivalent platinum species were in the modified TiO_2. The peaks of $Pt_{4f}7/2$ and $Pt_{4f}5/2$ at 70.7 and 74.0 eV were referred to metallic Pt^0, those peaks at 72.3 and 75.7 eV from Pt^{2+}, and those peaks at 73.6 and 76.8 eV from Pt^{4+} [50-52]. The overall Pt loading was estimated to be 1.42 at.%, corresponding to a Pt/Ti ratio of 1/23.14, which was higher than designed ratio of 1/33. Based on the peak area, the relative percentages of multivalent platinum in doped Pt were obtained as 1.17 at.% for Pt^0, 97.21 at.% for Pt^{2+}, and 1.62 at.% for Pt^{4+}. Only Pt^{4+} has a similar ion radius to Ti^{4+} to be doped at substitutional sites. The oxidised states of platinum in the sample were either PtO_x, $PtNO_y$ or $PtCl_z$, due to the mild calcination [41]. These species therefore would be located onto the surface of the particles and play as centres to absorb visible light for a higher photocatalytic activity. Moreover, Pt^0 can also act as a cocatalyst to accelerate photoinduced carriers' separation rate for an enhanced photocatalytic activity.

3.5. Photocatalytic oxidation of phenol solutions

3.5.1. Effect of dopants on the photocatalytic activity

Fig. 5(A) shows the photodegradation of phenol under UV-visible (UV-vis) irradiations. A control experiment showed that photolysis without a photocatalyst could hardly decompose phenol. The prepared TiO_2 showed a medium activity under UV-vis irradiations, providing 35.6% phenol degradation at 120 min. Degussa P25 showed a higher activity than the prepared TiO_2, due to the higher crystallinity and mixed crystalline phases of anatase and rutile. The phenol degradation rate by P25 reached 63.9% at 120 min. That was also higher than N-TiO_2 (41.9%), because UV activity was dominant to the enhanced proportion of N-TiO_2 from visible light. But in comparison between pure TiO_2 and N-TiO_2 from the similar preparation, an enhancement in activity of N-TiO_2 was observed, owing to the visible activity from N-doping [15]. In the codoped samples the doping level of metal was consistent at 1.0

at.%. N-Fe- and N-Ni-codoped TiO_2 showed even a lower activity than N-TiO_2, though band gap energies of them were greatly decreased (Fig. 3). However, high visible light absorption does not secure a high visible light photocatalytic activity. Table 1 indicates that the distortion from nitrogen and transition metal codoping was very high, the decreased activity was possibly ascribed to the higher distortion level, which increased the recombination rate of photoinduced carriers. Yin et al. [36] observed a positive synergistic effect of nitrogen and iron codoping, where Fe doping level was 0.5 wt.% based on Fe_2O_3 (Fe 0.17 at.%). Wu et al. [53] investigated carbon and iron modified TiO_2 and found that the doping level of Fe would significantly influence the photocatalytic activity and sample with Fe 0.57 mol% (0.19 at.%) showed the highest efficiency. Zhang et al. [34] also showed that N(0.01)-Ni(0.015)-TiO_2 (Ni 0.5 at.%) had a very high photocatalytic activity. Low efficiency of nitrogen and transition metal codoped TiO_2 in this work might be attributed to a higher doping level (1.0 at.%).

[Insert Fig. 5]

Nevertheless, noble metals (Ag and Pt) showed positive performances at this doping level with nitrogen in codoped TiO_2 photocatalysts. Both N-Ag- and N-Pt-codoped TiO_2 were more effective than N-TiO_2. N-Ag-TiO_2 was able to degrade 51.3% of phenol in 120 min, compared to 41.9% of N-TiO_2. N-Pt-TiO_2 showed outstanding performance and was able to completely decompose 20 ppm of phenol in 60 min. In general, photodegradation of phenol can be described by the Langmuir-Hinshelwood mechanism, and first-order kinetics can be applied [14]. The apparent-reaction-rate constants of P25, N-TiO_2, N-Ag-TiO_2 and N-Pt-TiO_2 were estimated as 8.76×10^{-3} ($R^2 = 0.995$), 4.51×10^{-3} ($R^2 = 0.999$), 5.60×10^{-3} ($R^2 = 0.993$), and 5.14×10^{-2} ($R^2 = 0.997$) min^{-1}, respectively. It was seen that N-Ag-TiO_2, though, was better than N-TiO_2, it was still inferior to P25. It was interesting to see that N-Pt-TiO_2 had a very high activity, almost 5.9 times as high as that of P25 under UV-vis irradiations. Fig. 4 (c) showed that multivalent platinum was present in N-Pt-TiO_2, according to ionic radii (Table 1), only Pt^{4+} (0.076 nm) is close to Ti^{4+} (0.068 nm), therefore most of platinum was loaded on the surface of modified TiO_2. The higher activity of N-Pt-TiO_2 was possibly because of the proper doping level and the surface groups serving as light absorbing centres. Moreover, zero-valent-platinum is also a centre for trapping electrons, resulting in a higher carriers'

separation rate as well as photocatalytic activity. In this case, Pt^0 plays the role of a cocatalyst on the surface of the photocatalyst. Therefore, we selected Pt as a model for further investigation of the synergistic effect of codoping.

3.5.2. Synergistic effect of nitrogen and platinum codoping

For N-, and/or Pt-modified TiO_2, we investigated the synergistic effect of single and codoping, as shown in Fig. 5(B). Except for N-TiO_2, all other samples, Pt-TiO_2 (Pt 1.0 at.%) and N-Pt-codoped TiO_2 showed a higher activity than P25 under UV-vis irradiations. In comparison of phenol degradation rate at 60 min, 22.2%, 73.6% and 100% in photocatalytic efficiencies were obtained on N-TiO_2, Pt-TiO_2 and N-Pt-TiO_2, respectively. The apparent-reaction-rate constants of the three photocatalysts were evaluated to be 4.51×10^{-3} ($R^2 = 0.999$), 2.44×10^{-2} ($R^2 = 0.989$) and 5.14×10^{-2} ($R^2 = 0.997$) min^{-1}, respectively. A synergistic effect between Pt and N doping was genuinely demonstrated.

The doping level of Pt significantly affected the phenol degradation rate. Both Pt 0.5 at.% and 1.0 at.% were able to dramatically increase the efficiency of N-TiO_2. Pt doping was found to be more effective than nitrogen doping in this study, but it was noted that N doping level was very low. Main interest of N-doping was to create a visible response, whereas an enhancement of UV activity from N-doping was not significant [5]. The minor change of UV activity is due to that less carriers' recombination centres are created by non-metal doping than transition metal doping [54]. In contrast, Pt doping would not only create visible light absorption but increase carriers' separation rate, resulting in enhancements of UV and visible light photocatalytic activity [55].

The synergistic effects of N and Pt codoping were experimentally confirmed as follows. (a) N doping improved the chemical states of platinum by minimising metallic Pt, as proven by XRD patterns (Fig. 1 (B)) and XPS spectra (Fig. 4 (C)). (b) Codoping of Pt increased N doping level from 0.21 at.% to 0.75 at.%. (c) The photodegradation reaction rate of 5.14×10^{-2} min^{-1} ($R^2 = 0.997$) on N-Pt-TiO_2 was much higher than the simple addition of rate from 4.51×10^{-3} min^{-1} ($R^2 = 0.999$) of N-TiO_2 and 2.44×10^{-2} min^{-1} ($R^2 = 0.989$) of Pt-TiO_2 under UV-visible light irradiations (Fig. 5 (A)).

3.5.3. Photodegradation of phenol under visible light

For the practical application, higher activity under UV-visible irradiations would lead to more effective utilization of natural sunlight. Therefore, we selected N-Pt-TiO_2, which shows the highest activity at UV-visible light, for further investigations under visible light irradiations. Fig. 6 (A) shows that all the doped and codoped TiO_2 showed higher activities than P25 under visible light ($\lambda > 430$ nm). Phenol degradation rates of N-, Pt (1.0 at.%)-, N-Pt (0.5 at.%)-TiO_2 at 360 min were 46.1, 100, and 84.7%, respectively. Whereas N-Pt (1.0 at.%)-TiO_2 was able to reach 100% phenol removal at 240 min. The apparent-reaction-rate constants of N-TiO_2, Pt-TiO_2 and N-Pt-TiO_2 under this irradiation were evaluated to be 1.68×10^{-3} ($R^2 = 0.998$), 9.33×10^{-3} ($R^2 = 0.997$) and 1.31×10^{-2} ($R^2 = 0.998$) min^{-1}, respectively. It was also found that Pt (1.0 at.%) showed even higher activity than N-Pt (0.5 at.%), indicating that platinum plays a more important role in improving the activity of modified TiO_2. That would be due to that platinum can be beneficial to both increasing visible light absorption by ions and improving carriers' separation by metallic Pt.

[Insert Fig. 6]

Fig. 6 (B) shows the activities of various photocatalysts under the irradiations with wavelength longer than 490 nm. Phenol degradation in 360 min by N-, Pt (1.0 at.%)-, N-Pt (0.5 at.%)-, and N-Pt (1.0 at.%)-TiO_2 was observed as 12.6, 44.0, 42.0, and 64.0%, respectively. The apparent-reaction-rate constants of N-TiO_2, Pt-TiO_2 and N-Pt-TiO_2 under this irradiation were evaluated to be 4.72×10^{-4} ($R^2 = 0.817$), 1.75×10^{-3} ($R^2 = 0.984$) and 3.16×10^{-3} ($R^2 = 0.988$) min^{-1}, respectively. UV-vis spectra (Fig. 3) showed that N-TiO_2 had a visible absorption up to 550 nm, and Pt codoping would extend the adsorption to whole visible light region. Therefore, it was plausible to observe visible light photocatalytic activity in current light wavelength region. The results confirmed that N-Pt-TiO_2 showed the highest activity among all the prepared photocatalysts and P25 under UV or vis irradiations.

3.5.4. Mechanism of photodegradation of phenol over N-Pt-TiO_2 under visible light

It was concluded that N and Pt would work together to significantly improve the optical properties and visible light photocatalytic activity of TiO_2. However, the mechanism of the

synergistic effect and the origin of visible light response of N-Pt-TiO_2 have not been conclusive, even for the single dopant of nitrogen or platinum. For example, substitutional N, NO_x, NH_x and oxygen vacancies have been proposed as the origin of visible light response of nitrogen doped TiO_2 [5, 14, 16, 41]. For Pt modified TiO_2, Mallat et al. [56] suggested that Pt^0 had the beneficial effect for catalytic oxidation of alcohol. Lee and Choi [57] reported that Pt^0 had a better effect than Pt^{2+} on TiO_2 for degradation of dichloroacetate, 4-chlorophenol and chloroform. But Wu et al. [58] found that Pt^0/TiO_2 and $PtCl_x/TiO_2$ hardly contributed to the enhanced photocatalytic oxidation of NO, while PtO_x/TiO_2 had a high activity. The controversies in both N doping and Pt modification make it difficult to provide a comprehensive and conclusive mechanism on visible light photocatalysis of N-Pt-TiO_2. Based on experimental results in this investigation, a tentative mechanism is proposed to illustrate the roles of dopants in visible light photocatalysis, as shown in Scheme 1. XPS studies shows N 1s peak at about 400 eV, indicating the formation of NO_x, which would not significantly reduce the band gap energy of TiO_2. The visible response was only from N impurity states, as confirmed by UV-vis DRS of N-TiO_2. XPS also shows that the dopant of platinum had at least three chemical states of 0, 2+ and 4+. Minor platinum doping could lower the conduction band of TiO_2. The metallic Pt particles was well known as an effective electron trap on the surface of TiO_2 to improve the separation efficiency of photogenerated electron-hole pairs, then to enhance the photocatalytic activity [45]. Pt^{2+} was the main platinum species in our sample. It was reported that PtO_x is a p-type semiconductor with a narrow band gap energy than the n-type semiconductor of TiO_2. The heterojunction of PtO_x-TiO_2 formed on the surface of TiO_2 was expected to accelerate the electron-hole separation rate [58]. Once $PtCl_z$ is formed, a Z-scheme mechanism for the charge separation could be applied. By above complicated ways, the visible light response and enhanced photocatalytic activity were obtained. The electron can react with oxygen in water forming superoxygen anions to oxidise the organic pollutants. The hole can also be trapped by water to produce an active hydroxyl radical, which is powerful oxidative species for oxidation of organics.

[Insert Scheme 1]

4. Conclusions

One-pot synthesis was applied to successfully prepare nitrogen and metal codoped titania photocatalysts. It was found that codoping by a metal to N-TiO_2 would significantly change the physicochemical properties. At a certain doping level of 1.0 at.%, the codoped metal ions also performed differently in degradation of aqueous organic pollutants, with improvements from noble metals (Ag or Pt) but deterioration by transition metals (Fe or Ni). Transition metal ions can be easily doped into TiO_2 crystal, therefore leading to new recombination centres of photoinduced carriers and a lower activity. While platinum can be present in two phases, ions and metallic nanoparticles, ensuring the higher activity than single N-doped TiO_2. The synergistic effect between N and Pt doping was also observed, attributed to the mixed states of platinum. Further studies can be carried out in two different ways: (a) comparative study of the photocatalysts with optimum doping level of each dopant, and (b) comparative study of photocatalysts at very low doping level of metals, such as 0.01 at.%. The further comprehensive studies in this field would be valuable for design and synthesis of novel metal-nonmetal codoped photocatalysts, and discovery of the insightful mechanism.

References

[1] M. Pelaez, N.T. Nolan, S.C. Pillai, M.K. Seery, P. Falaras, A.G. Kontos, P.S.M. Dunlop, J.W.J. Hamilton, J.A. Byrne, K. O'Shea, M.H. Entezari, D.D. Dionysiou, A review on the visible light active titanium dioxide photocatalysts for environmental applications, Appl. Catal. B, 125 (2012) 331-349.

[2] R. Daghrir, P. Drogui, D. Robert, Modified TiO_2 For Environmental Photocatalytic Applications: A Review, Ind. Engin. Chem. Res., 52 (2013) 3581-3599.

[3] E. Grabowska, J. Reszczynska, A. Zaleska, Mechanism of phenol photodegradation in the presence of pure and modified-TiO_2: A review, Wat. Res., 46 (2012) 5453-5471.

[4] S. Sato, Photocatalytic activity of NO_x-doped TiO_2 in the visible-light region, Chem. Phys. Lett., 123 (1986) 126-128.

[5] R. Asahi, T. Morikawa, T. Ohwaki, K. Aoki, Y. Taga, Visible-light photocatalysis in nitrogen-doped titanium oxides, Science, 293 (2001) 269-271.

[6] D. Dvoranova, V. Brezova, M. Mazur, M.A. Malati, Investigations of metal-doped titanium dioxide photocatalysts, Appl. Catal. B, 37 (2002) 91-105.

[7] M.I. Litter, J.A. Navio, Photocatalytic properties of iron-doped titania semiconductors, J. Photochem. Photobiol. A, 98 (1996) 171-181.

[8] S. Sato, Photocatalysts sensitive to visible light, Science, 295 (2002) 626-627.

[9] T. Morikawa, R. Asahi, T. Ohwaki, K. Aoki, Y. Taga, Band-gap narrowing of titanium dioxide by nitrogen doping, Jap. J. Appl. Phys. 2-Lett., 40 (2001) L561-L563.

[10] Z.B. Wu, F. Dong, W.R. Zhao, S. Guo, Visible light induced electron transfer process over nitrogen doped TiO_2 nanocrystals prepared by oxidation of titanium nitride, J. Hazard. Mater., 157 (2008) 57-63.

[11] Y.C. Hong, C.U. Bang, D.H. Shin, H.S. Uhm, Band gap narrowing of TiO_2 by nitrogen doping in atmospheric microwave plasma, Chem. Phys. Lett., 413 (2005) 454-457.

[12] A. Kafizas, I.P. Parkin, The combinatorial atmospheric pressure chemical vapour deposition (cAPCVD) of a gradating N-doped mixed phase titania thin film, J. Mater. Chem., 20 (2010) 2157-2169.

[13] Y.M. Wu, H.B. Liti, J.L. Zhang, F. Chen, Enhanced Photocatalytic Activity of Nitrogen-Doped Titania by Deposited with Gold, J. Phys. Chem. C, 113 (2009) 14689-14695.

[14] H.Q. Sun, Y. Bai, W.Q. Jin, N.P. Xu, Visible-light-driven TiO_2 catalysts doped with low-concentration nitrogen species, Sol. Energy Mater. Sol. Cells, 92 (2008) 76-83.

[15] H.Q. Sun, Y. Bai, H.J. Liu, W.Q. Jin, N.P. Xu, Photocatalytic decomposition of 4-chlorophenol over an efficient N-doped TiO_2 under sunlight irradiation, J. Photochem. Photobiol. A, 201 (2009) 15-22.

[16] H.Q. Sun, Y. Bai, H.J. Liu, W.Q. Jin, N.P. Xu, G.J. Chen, B.Q. Xu, Mechanism of nitrogen-concentration dependence on pH value: Experimental and theoretical studies on nitrogen-doped TiO_2, J. Phys. Chem. C, 112 (2008) 13304-13309.

[17] T.C. Jagadale, S.P. Takale, R.S. Sonawane, H.M. Joshi, S.I. Patil, B.B. Kale, S.B. Ogale, N-doped TiO_2 nanoparticle based visible light photocatalyst by modified peroxide sol-gel method, J. Phys. Chem. C, 112 (2008) 14595-14602.

[18] D.G. Huang, S.J. Liao, S.Q. Quan, L. Liu, Z.J. He, J.B. Wan, W.B. Zhou, Synthesis and characterization of visible light responsive N-TiO_2 mixed crystal by a modified hydrothermal process, J. Non-Cryst. Solids, 354 (2008) 3965-3972.

[19] J.J. Liu, W. Qin, S.L. Zuo, Y.C. Yu, Z.P. Hao, Solvothermal-induced phase transition and visible photocatalytic activity of nitrogen-doped titania, J. Hazard. Mater., 163 (2009) 273-278.

[20] S. Livraghi, M.C. Paganini, E. Giamello, A. Selloni, C. Di Valentin, G. Pacchioni, Origin of photoactivity of nitrogen-doped titanium dioxide under visible light, J. Am. Chem.

Soc., 128 (2006) 15666-15671.
[21] D. Mitoraj, H. Kisch, The Nature of Nitrogen-Modified Titanium Dioxide Photocatalysts Active in Visible Light, Angew. Chem. Inter. Ed., 47 (2008) 9975-9978.
[22] C. Burda, Y.B. Lou, X.B. Chen, A.C.S. Samia, J. Stout, J.L. Gole, Enhanced nitrogen doping in TiO_2 nanoparticles, Nano Lett., 3 (2003) 1049-1051.
[23] O. Diwald, T.L. Thompson, T. Zubkov, E.G. Goralski, S.D. Walck, J.T. Yates, Photochemical activity of nitrogen-doped rutile TiO_2(111) in visible light, J. Phys. Chem. B, 108 (2004) 6004-6008.
[24] T. Ihara, M. Miyoshi, Y. Iriyama, O. Matsumoto, S. Sugihara, Visible-light-active titanium oxide photocatalyst realized by an oxygen-deficient structure and by nitrogen doping, Appl. Catal. B, 42 (2003) 403-409.
[25] S. Sakthivel, M. Janczarek, H. Kisch, Visible light activity and photoelectrochemical properties of nitrogen-doped TiO_2, J. Phys. Chem. B, 108 (2004) 19384-19387.
[26] M. Sathish, B. Viswanathan, R.P. Viswanath, C.S. Gopinath, Synthesis, characterization, electronic structure, and photocatalytic activity of nitrogen-doped TiO_2 nanocatalyst, Chem. Mater., 17 (2005) 6349-6353.
[27] X.B. Chen, Y.B. Lou, A.C.S. Samia, C. Burda, J.L. Gole, Formation of oxynitride as the photocatalytic enhancing site in nitrogen-doped titania nanocatalysts: Comparison to a commercial nanopowder, Adv. Funct. Mater., 15 (2005) 41-49.
[28] H.Q. Sun, Y. Bai, Y.P. Cheng, W.Q. Jin, N.P. Xu, Preparation and characterization of visible-light-driven carbon-sulfur-codoped TiO_2 photocatalysts, Ind. Engin. Chem. Res., 45 (2006) 4971-4976.
[29] D. Li, H. Haneda, S. Hishita, N. Ohashi, Visible-light-driven N-F-codoped TiO_2 photocatalysts. 2. Optical characterization, photocatalysis, and potential application to air purification, Chem. Mater., 17 (2005) 2596-2602.
[30] P. Periyat, D.E. McCormack, S.J. Hinder, S.C. Pillai, One-Pot Synthesis of Anionic (Nitrogen) and Cationic (Sulfur) Codoped High-Temperature Stable, Visible Light Active, Anatase Photocatalysts, J. Phys. Chem. C, 113 (2009) 3246-3253.
[31] B. Naik, K.M. Parida, C.S. Gopinath, Facile Synthesis of N- and S-Incorporated Nanocrystalline TiO_2 and Direct Solar-Light-Driven Photocatalytic Activity, J. Phys. Chem. C, 114 (2010) 19473-19482.
[32] X.P. Wang, T.T. Lim, Solvothermal synthesis of C-N codoped TiO_2 and photocatalytic evaluation for bisphenol A degradation using a visible-light irradiated LED photoreactor, Appl. Catal. B, 100 (2010) 355-364.
[33] Y.G. Sheng, Y. Xu, D. Jiang, L.P. Liang, D. Wu, Y.H. Sun, Hydrothermal preparation of visible-light-driven N-Br-codoped TiO_2 photocatalysts, Inter. J. Photoenergy, (2008).
[34] X. Zhang, Q.Q. Liu, Visible-light-induced degradation of formaldehyde over titania photocatalyst co-doped with nitrogen and nickel, Appl. Surf. Sci., 254 (2008) 4780-4785.

[35] B. Naik, K.M. Parida, Solar Light Active Photodegradation of Phenol over a $Fe_xTi_{1-x}O_{2-y}N_y$ Nanophotocatalyst, Ind. Engin. Chemistry Res., 49 (2010) 8339-8346.

[36] S. Yin, B. Liu, P.L. Zhang, T. Morikawa, K. Yamanaka, T. Sato, Photocatalytic oxidation of NOx under visible LED light irradiation over nitrogen-doped titania particles with iron or platinum loading, J. Phys. Chem. C, 112 (2008) 12425-12431.

[37] T. Morikawa, T. Ohwaki, K.I. Suzuki, S. Moribe, S. Tero-Kubota, Visible-light-induced photocatalytic oxidation of carboxylic acids and aldehydes over N-doped TiO_2 loaded with Fe, Cu or Pt, Appl. Catal. B, 83 (2008) 56-62.

[38] T. Sreethawong, S. Laehsalee, S. Chavadej, Use of Pt/N-doped mesoporous-assembled nanocrystalline TiO_2 for photocatalytic H-2 production under visible light irradiation, Catal. Commun., 10 (2009) 538-543.

[39] G. Halasi, G. Schubert, F. Solymosi, Comparative study on the photocatalytic decomposition of methanol on TiO_2 modified by N and promoted by metals, J. Catal., 294 (2012) 199-206.

[40] P.G. Wu, R.C. Xie, K. Imlay, J.K. Shang, Visible-Light-Induced Bactericidal Activity of Titanium Dioxide Codoped with Nitrogen and Silver, Environ. Sci. Technol., 44 (2010) 6992-6997.

[41] H.Q. Sun, R. Ullah, S.H. Chong, H.M. Ang, M.O. Tade, S.B. Wang, Room-light-induced indoor air purification using an efficient Pt/N-TiO_2 photocatalyst, Appl. Catal. B, 108 (2011) 127-133.

[42] I. Djerdj, A.M. Tonejc, Structural investigations of nanocrystalline TiO_2 samples, J. Alloy. Compd., 413 (2006) 159-174.

[43] K.M. Parida, B. Naik, Synthesis of mesoporous $TiO_{2-x}N_x$ spheres by template free homogeneous co-precipitation method and their photo-catalytic activity under visible light illumination, J. Coll. Interf. Sci., 333 (2009) 269-276.

[44] S. Yamazaki, Y. Fujiwara, S. Yabuno, K. Adachi, K. Honda, Synthesis of porous platinum-ion-doped titanium dioxide and the photocatalytic degradation of 4-chlorophenol under visible light irradiation, Appl. Catal. B, 121 (2012) 148-153.

[45] D.Z. Li, Z.X. Chen, Y.L. Chen, W.J. Li, H.J. Huang, Y.H. He, X.Z. Fu, A new route for degradation of volatile organic compounds under visible light: Using the bifunctional photocatalyst Pt/$TiO_{2-x}N_x$ in H_2O_2 atmosphere, Environ. Sci. Technol., 42 (2008) 2130-2135.

[46] H.Q. An, J. Zhou, J.X. Li, B.L. Zhu, S.R. Wang, S.M. Zhang, S.H. Wu, W.P. Huang, Deposition of Pt on the stable nanotubular TiO_2 and its photocatalytic performance, Catal. Commun., 11 (2009) 175-179.

[47] G.L. Zhou, H.Q. Sun, S.B. Wang, H.M. Ang, M.O. Tade, Titanate supported cobalt catalysts for photochemical oxidation of phenol under visible light irradiations, Sep. Purif. Technol., 80 (2011) 626-634.

[48] S. Higashimoto, Y. Ushiroda, M. Azuma, H. Ohue, Synthesis, characterization and

photocatalytic activity of N-doped TiO_2 modified by platinum chloride, Catal. Tod., 132 (2008) 165-169.

[49] M. Miyauchi, M. Takashio, H. Tobimatsu, Photocatalytic activity of $SrTiO_3$ codoped with nitrogen and lanthanum under visible light illumination, Langmuir, 20 (2004) 232-236.

[50] V. Iliev, D. Tomova, L. Bilyarska, A. Eliyas, L. Petrov, Photocatalytic properties of TiO_2 modified with platinum and silver nanoparticles in the degradation of oxalic acid in aqueous solution, Appl. Catal. B, 63 (2006) 266-271.

[51] E.A. Kozlova, T.P. Lyubina, M.A. Nasalevich, A.V. Vorontsov, A.V. Miller, V.V. Kaichev, V.N. Parmon, Influence of the method of platinum deposition on activity and stability of Pt/TiO_2 photocatalysts in the photocatalytic oxidation of dimethyl methylphosphonate, Catal. Commun., 12 (2011) 597-601.

[52] Z.B. Wu, Z.Y. Sheng, Y. Liu, H.Q. Wang, J.S. Mo, Deactivation mechanism of PtO_x/TiO_2 photocatalyst towards the oxidation of NO in gas phase, J. Hazard. Mater., 185 (2011) 1053-1058.

[53] Y.M. Wu, J.L. Zhang, L. Xiao, F. Chen, Properties of carbon and iron modified TiO_2 photocatalyst synthesized at low temperature and photodegradation of acid orange 7 under visible light, Appl. Surf. Sci., 256 (2010) 4260-4268.

[54] J.F. Zhu, W. Zheng, H.E. Bin, J.L. Zhang, M. Anpo, Characterization of $Fe\text{-}TiO_2$ photocatalysts synthesized by hydrothermal method and their photocatalytic reactivity for photodegradation of XRG dye diluted in water, J. Mol. Catal., 216 (2004) 35-43.

[55] E. Kowalska, H. Remita, C. Colbeau Justin, J. Hupka, J. Belloni, Modification of titanium dioxide with platinum ions and clusters: Application in photocatalysis, J. Phys. Chem. C, 112 (2008) 1124-1131.

[56] T. Mallat, A. Baiker, Oixdation of Alcohols with molecular-oxygenon platnium metal-catalysts in aqueous-solutions, Catal. Tod., 19 (1994) 247-283.

[57] J.S. Lee, W.Y. Choi, Photocatalytic reactivity of surface platinized TiO_2: Substrate specificity and the effect of Pt oxidation state, J. Phys. Chem. B, 109 (2005) 7399-7406.

[58] H.Q. Wang, Z.B. Wu, Y. Liu, Y.J. Wang, Influences of various Pt dopants over surface platinized TiO_2 on the photocatalytic oxidation of nitric oxide, Chemosphere, 74 (2009) 773-778.

Table 1 Crystallite size, lattice parameters, and doping levels of various photocatalysts and ion radii of their dopants.

Sample	Crystallite size/ nm	Lattice parameters /Å	Level and chemical states of dopants	Changes in *c* axis /Å	Ion radii /nm
Undoped TiO_2	6.4	a=b=3.7800 c=9.5007	/	--	Ti^{4+}: 0.068 O^{2-}: 0.124
N-TiO_2	6.9	a=b=3.7814 c=9.4922	N^{2-} (0.21 at.%)	-0.0085	N^{2-}: -
N-Fe-TiO_2	5.3	a=b=3.7830 c=9.4844	N^{2-}, Fe^{3+}	-0.0163	Fe^{2+}:0.074 Fe^{3+}: 0.064
N-Ni-TiO_2	5.6	a=b=3.7831 c=9.4824	N^{2-}, Ni^{2+}	-0.0183	Ni^{2+}: 0.078 Ni^{3+}: 0.066
N-Ag-TiO_2	5.9	a=b=3.7840 c=9.4925	N^{2-} (0.44 at.%), Ag^0 (99.65 at.%), Ag^{1+} (0.35 at.%)	-0.0082	Ag^{1+}: 0.129
N-Pt (1.0 at.%)-TiO_2	5.1	a=b=3.7791 c=9.4628	N^{2-}, Pt^0, Pt^{2+}, Pt^{4+},	-0.0379	Pt^{2+}: 0.080 Pt^{4+}: 0.063
N-Pt (0.5 at.%)-TiO_2	4.8	a=b=3.7800 c=9.4938	N^{2-}, Pt^0, Pt^{2+}, Pt^{4+},	-0.0069	As above
Pt (1.0 at.%)-TiO_2	5.7	a=b=3.7806 c=9.4853	N^{2-} (0.75 at.%), Pt^0 (1.17 at.%), Pt^{2+} (97.21 at.%), Pt^{4+} (1.62 at.%)	-0.0154	As above

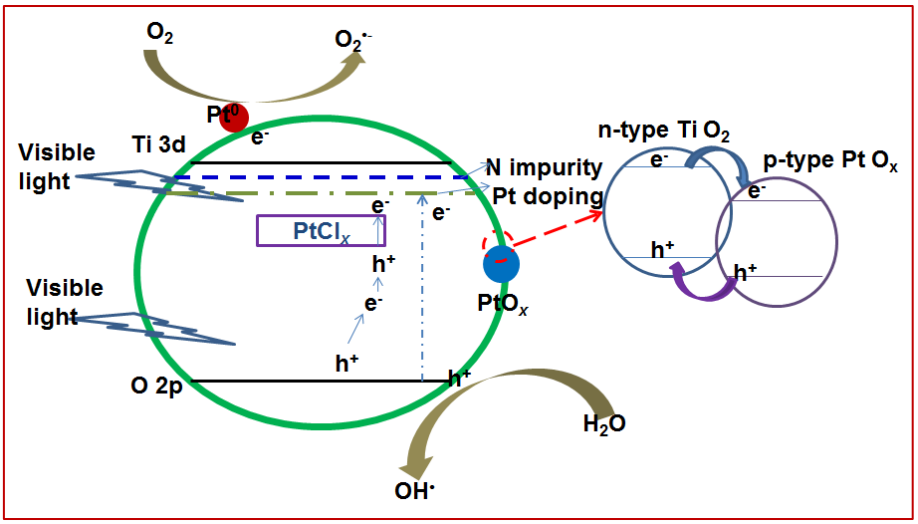

Scheme 1 Schematic diagram of N-Pt-TiO_2 photocatalysis under visible light irradiations.

List of Figure Captions

Figure 1 XRD patterns of (a) Pure TiO_2, (b) N-TiO_2, (c) N-Fe-TiO_2, (d) N-Ni-TiO_2, (e) N-Ag-TiO_2, and (f) N-Pt-TiO_2 for (A); and (i) Pt (1 at.%)-TiO_2, (ii) N-Pt (0.5 at.%)-TiO_2, and (iii) N-Pt (1.0 at.%)-TiO_2 for (B).

Figure 2 Nitrogen adsorption-desorption isotherms (A) and pore size distribution (B) of pure, N-doped, and N-Pt codoped TiO_2 photocatalysts.

Figure 3 UV-visible diffuse reflectance absorption spectra (A) and evaluations of band gap energies by Kubelka-Munk equations (B) of various photocatalysts.

Figure 4 XPS spectra of N 1*s* (A), Ti 2*p* (B) and Pt 4*f* (C) of various photocatalysts.

Figure 5 Photodegradation of phenol solutions under UV-visible lights, (A): Effect of dopants (a) without a photocatalyst, (b) prepared pure TiO_2, (c) Degussa P25, (d) N-TiO_2, (e) N-Fe-TiO_2, (f) N-Ni-TiO_2, (g) N-Ag-TiO_2, and (h) N-Pt-TiO_2; (B) Effect of dopants and doping level on photodegradation of phenol solutions under UV-visible light using (a) Degussa P25, (b) N-TiO_2, (c) Pt (1.0 at.%)-doped TiO_2, (d) N-Pt (0.5 at.%)-codoped TiO_2, and (e) N-Pt (1.0 at.%)-codoped TiO_2

Figure 6 Photodegradation of phenol solutions under visible light using (a) Degussa P25, (b) N-TiO_2, (c) Pt (1.0 at.%)-doped TiO_2, (d) N-Pt (0.5 at.%)-codoped TiO_2, and (e) N-Pt (1.0 at.%)-codoped TiO_2.

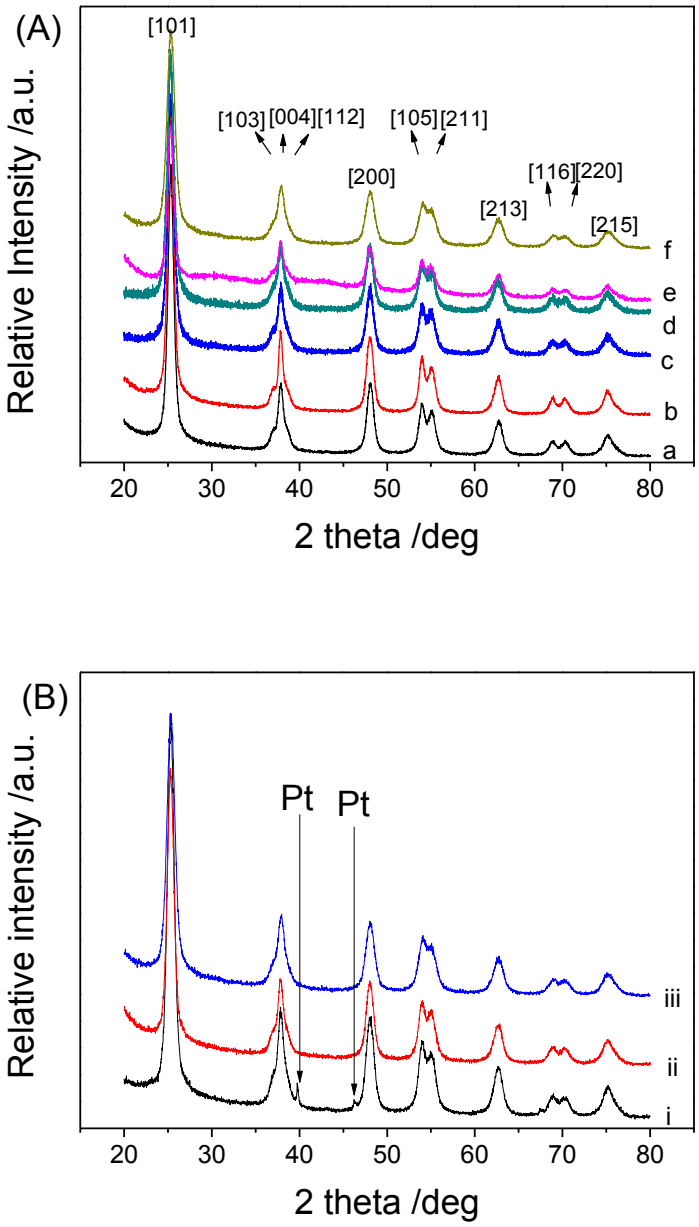

Figure 1 XRD patterns of (a) Pure TiO_2, (b) N-TiO_2, (c) N-Fe-TiO_2, (d) N-Ni-TiO_2, (e) N-Ag-TiO_2, and (f) N-Pt-TiO_2 for (A); and (i) Pt (1 at.%)-TiO_2, (ii) N-Pt (0.5 at.%)-TiO_2, and (iii) N-Pt (1.0 at.%)-TiO_2 for (B).

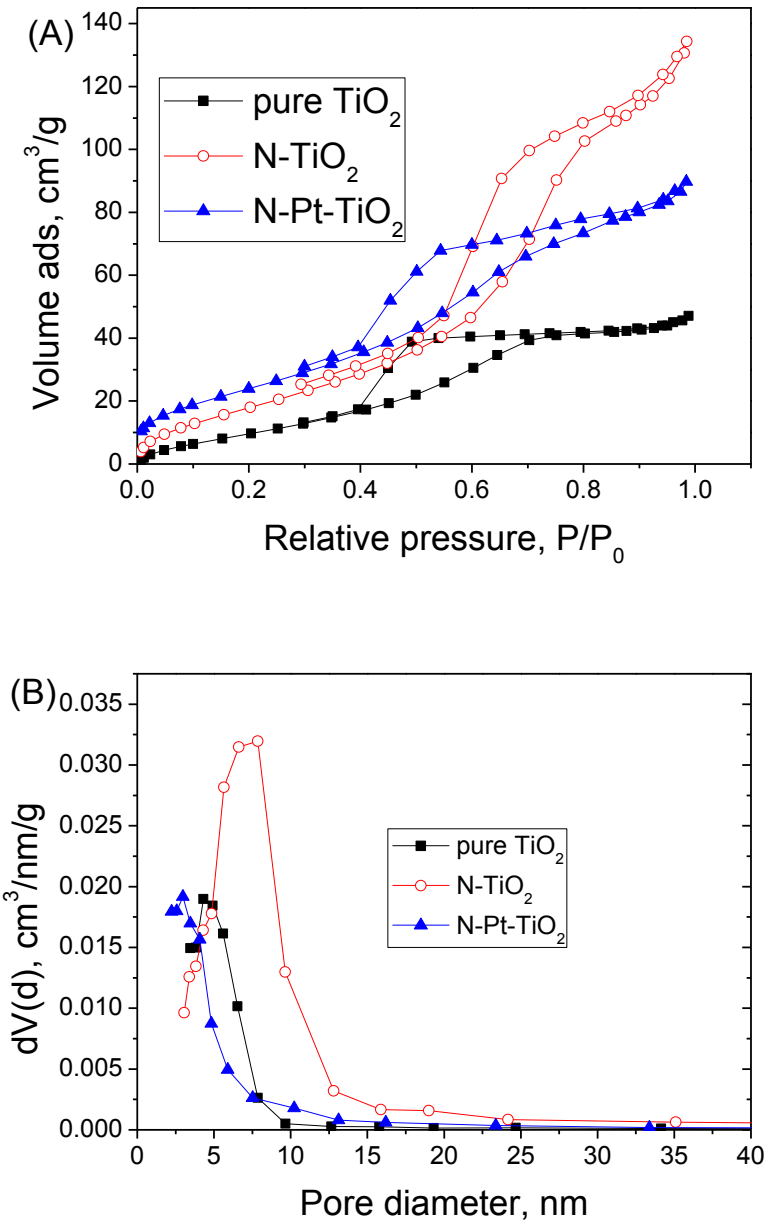

Figure 2 Nitrogen adsorption-desorption isotherms (A) and pore size distribution (B) of pure, N-doped, and N-Pt codoped TiO_2 photocatalysts

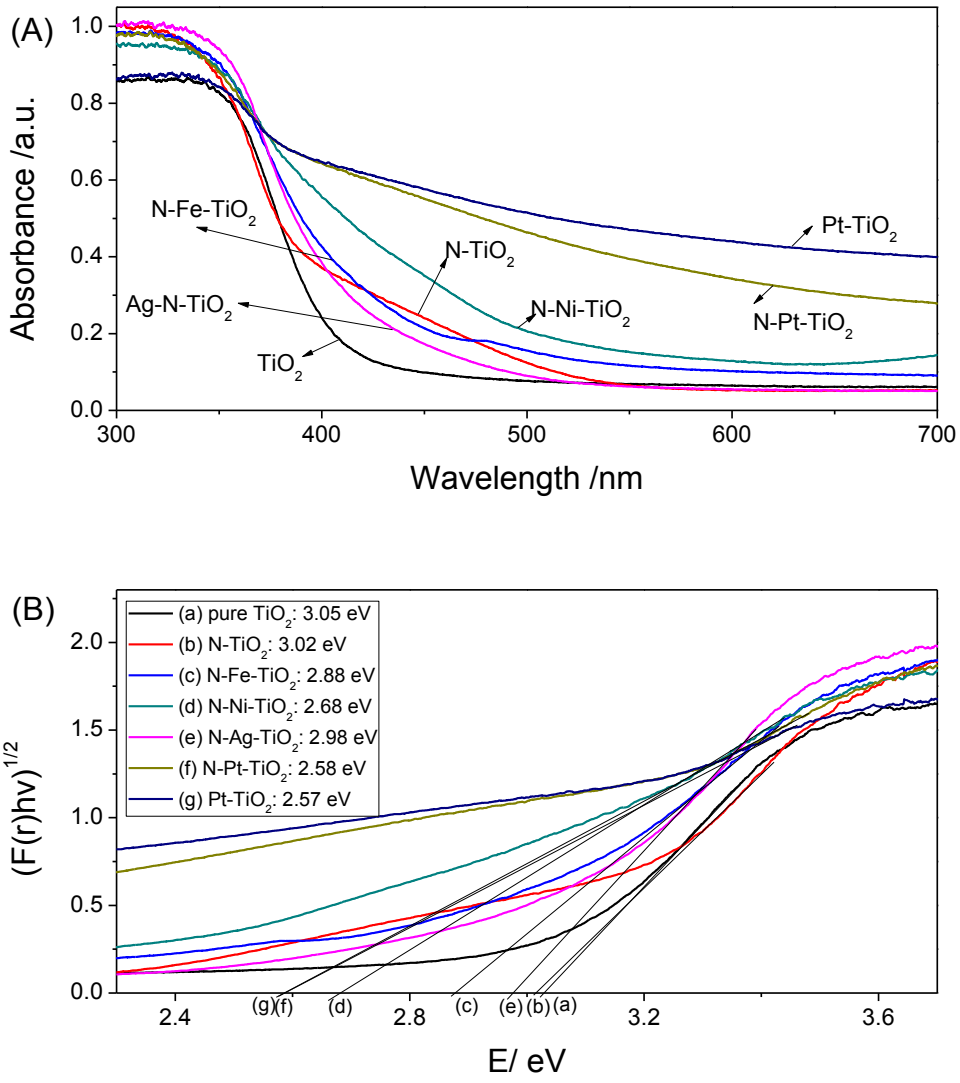

Figure 3 UV-visible diffuse reflectance absorption spectra (A) and evaluations of band gap energies by Kubelka-Munk equations (B) of various photocatalysts.

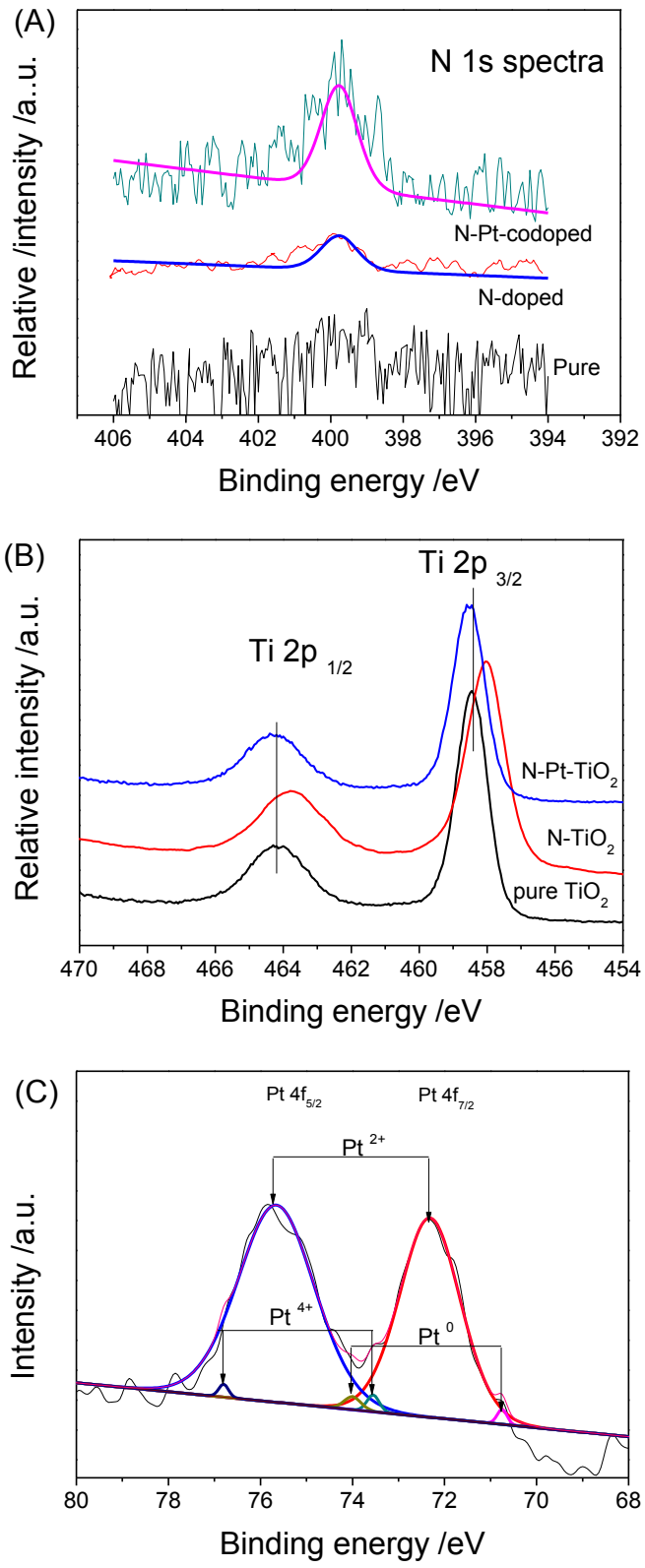

Figure 4 XPS spectra of N 1*s* (A), Ti 2*p* (B) and Pt 4*f* (C) of various photocatalysts

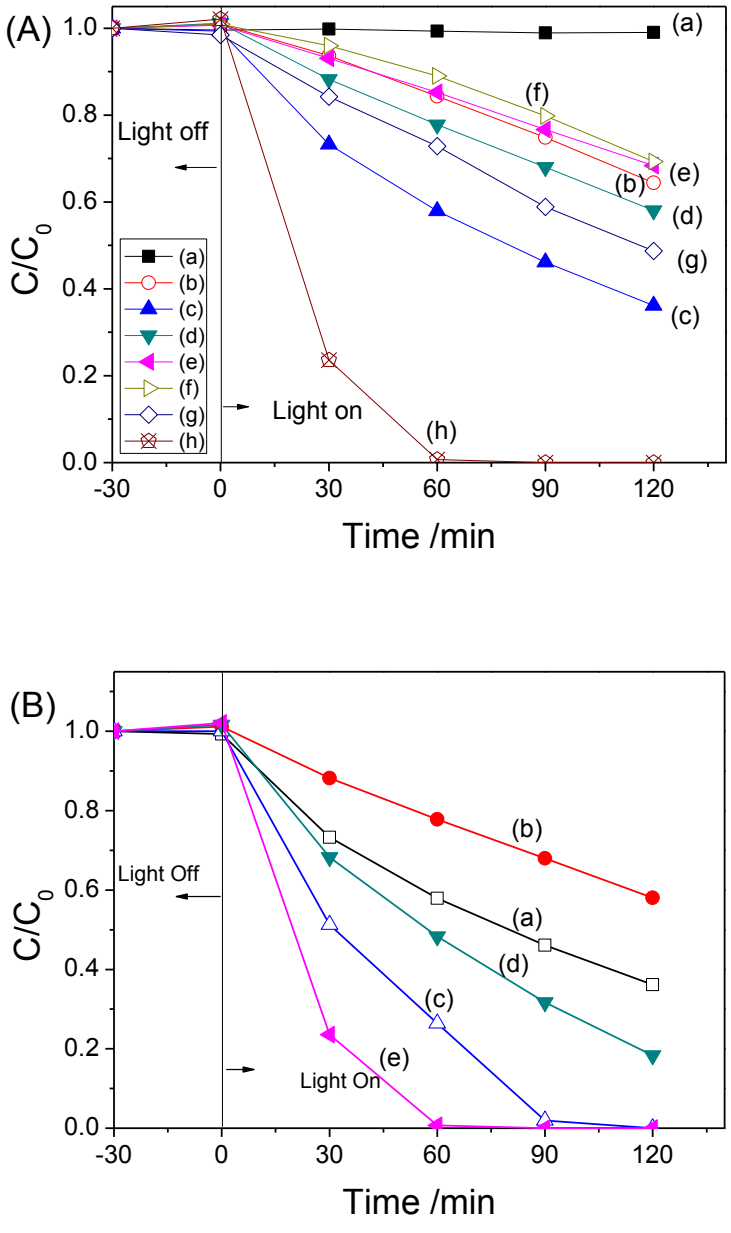

Figure 5 Photodegradation of phenol solutions under UV-visible lights, (A): Effect of dopants (a) without a photocatalyst, (b) prepared pure TiO_2, (c) Degussa P25, (d) N-TiO_2, (e) N-Fe-TiO_2, (f) N-Ni-TiO_2, (g) N-Ag-TiO_2, and (h) N-Pt-TiO_2; (B) Effect of dopants and doping level on photodegradation of phenol solutions under UV-visible light using (a) Degussa P25, (b) N-TiO_2, (c) Pt (1.0 at.%)-doped TiO_2, (d) N-Pt (0.5 at.%)-codoped TiO_2, and (e) N-Pt (1.0 at.%)-codoped TiO_2

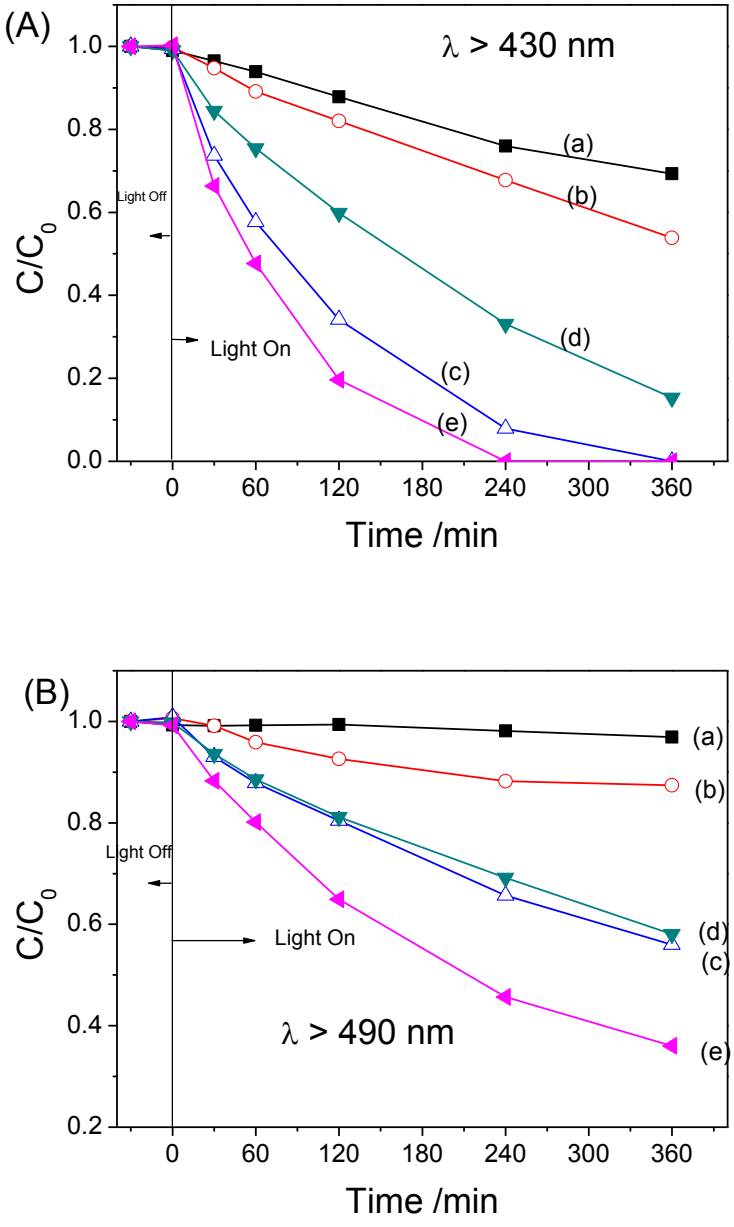

Figure 6 Photodegradation of phenol solutions under visible light using (a) Degussa P25, (b) N-TiO_2, (c) Pt (1.0 at.%)-doped TiO_2, (d) N-Pt (0.5 at.%)-codoped TiO_2, and (e) N-Pt (1.0 at.%)-codoped TiO_2